Received: 1 March 2021 | Revised: 23 June 2021 | Accepted: 25 June 2021

DOI: 10.1002/ardp.202100081

FULL PAPER

ARCH PHARM DPhG
Archiv der Pharmazie

Leishmanicidal and cytotoxic activities and 4D-QSAR of 2-arylidene indan-1,3-diones

Ana P. M. de Souza[1] | Maria C. A. Costa[2] | Alex R. de Aguiar[1] | Gustavo C. Bressan[3] | Graziela D. de Almeida Lima[4] | Wallace P. Lima[3,5] | Maria P. G. Borsodi[5] | Bartira R. Bergmann[5] | Márcia M. C. Ferreira[2] | Róbson R. Teixeira[1]

[1]Departamento de Química, Universidade Federal de Viçosa, Viçosa, Brazil

[2]Theoretical and Applied Chemometrics Laboratory (LQTA), Institute of Chemistry, University of Campinas, Campinas, Brazil

[3]Escola de Ciências da Saúde, Universidade do Grande Rio, Duque de Caxias, Brazil

[4]Departamento de Bioquímica e Biologia Molecular, Universidade Federal de Viçosa, Viçosa, Brazil

[5]Instituto de Biofísica Carlos Chagas Filho, Universidade Federal do Rio de Janeiro, Rio de Janeiro, Brazil

Correspondence
Róbson R. Teixeira, Departamento de Química, Universidade Federal de Viçosa, Av. P. H. Rolfs, S/N, Viçosa-MG 36570-900, Brazil.
Email: robsonr.teixeira@ufv.br

Abstract

The indan-1,3-dione and its derivatives are important building blocks in organic synthesis and present important biological activities. Herein, the leishmanicidal and cytotoxicity evaluation of 16 2-arylidene indan-1,3-diones is described. The compounds were evaluated against the leukemia cell lines HL60 and Nalm6, and the most effective ones were 2-(4-nitrobenzylidene)-1*H*-indene-1,3(2*H*)-dione (**4**) and 4-[(1,3-dioxo-1*H*-inden-2(3*H*)-ylidene)methyl]benzonitrile (**10**), presenting IC_{50} values of around 30 μmol/L against Nalm6. The leishmanicidal activity was assessed on *Leishmania amazonensis*, with derivative **4** (IC_{50} = 16.6 μmol/L) being the most active. A four-dimensional quantitative structure–activity analysis (4D-QSAR) was applied to the indandione derivatives, through partial least-squares regression. The statistics presented by the regression models built with the selected field descriptors of Coulomb (C) and Lennard-Jones (L) nature, considering the activities against *L. amazonensis*, HL60, and Nalm6 leukemia cells, were, respectively, R^2 = 0.88, 0.92, and 0.98; Q^2 = 0.83, 0.88, and 0.97. The presence of positive Coulomb descriptors near the carbonyl groups indicates that these polar groups are related to the activities. Besides, the presence of positive Lennard-Jones descriptors close to substituents R^3 or R^1 indicates that bulky nonpolar substituents in these positions tend to increase the activities. This study provides useful insights into the mode of action of indandione derivatives for each biological activity involved.

KEYWORDS

2-arylidene indan-1,3-diones, 4D-QSAR, cytotoxic activity, indan-1,3-dione, leishmanicidal activity

1 | INTRODUCTION

Leishmaniases and cancer are serious diseases that affect humans and are of great importance in terms of public health. Leishmaniases are a group of parasitic infections in which the etiologic agents are at least 20 species of the genus *Leishmania*.[1] It is estimated that leishmaniases affect 350 million people in 98 countries, with a global incidence of 0.9–1.6 million cases per year.[2] The parasites are transmitted to humans through the bite of female mosquitoes in the sand fly subfamily. The vast majority of leishmaniasis cases are

associated with the poorest human population, which is in a state of malnutrition and presents a weak immune system. In addition to these, other aggravating factors can be considered such as precarious housing, lack of financial resources, displacement of population, and environmental changes.[3] The clinical manifestations of leishmaniases include cutaneous, visceral, and mucocutaneous.[3] The first-line drugs for the treatment of leishmaniases are pentavalent antimonials.[4] Nevertheless, there are disadvantages related to them, such as the occurrence of serious side effects and a high incidence of disease recurrence.[5] There are alternative medicines, such as pentamidine, miltefosine, amphotericin B, and paromomycin. However, they present, among others, high toxicity, high resistance, teratogenicity, and ototoxicity.[6–10]

Cancer is the term given to more than 277 related diseases in which cells that have lost the ability to self-regulate proliferate without control, can invade adjacent tissues and organs, or can even spread to other parts of the body through the blood and lymphatic systems, giving rise to new tumor sites (i.e., metastasis).[11] It is the second leading cause of death worldwide (https://www.cancer.gov/about-cancer/understanding/what-is-cancer) and can have several causes including lifestyle habits, genetics, carcinogens, and environmental factors.[12] Cancer treatment involves radiotherapy, surgery, chemotherapy, immunotherapy, targeted therapy, hormone therapy, stem cell transplant, and precision medicine (https://www.cancer.gov/about-cancer/treatment/types). In terms of chemotherapy, there are several available drugs for cancer treatment. However, these drugs present several side effects (https://www.cancer.org/treatment/treatments-and-side-effects/treatment-types/chemotherapy/chemotherapy-side-effects.html), and there is also the development of cancer cell line resistance to the available drugs.[13] The resistance is related to the complex cell signaling pathways modulating the proliferation and ability of cancer cell lines to escape from apoptotic processes.

Given the problems aforementioned related to the available chemotherapy for leishmaniasis and cancer, the necessity for the search and development of new agents that could overcome these disadvantages is clear.

The indan-1,3-dione is an aromatic bicyclic β-diketone that was first synthesized more than a century ago.[14] This compound and its derivatives are valuable synthetic precursors that have been widely applied for the production of dyes,[15] semiconductors,[16] heterocycles,[17,18] and pharmaceuticals.[19] Indan-1,3-dione derivatives present several biological activities such as antitumoral,[20] anticoagulant,[21] anti-inflammatory,[22,23] neuroprotective,[24] and antimicrobial.[25] Besides, compounds presenting the indan-1,3-dione core have been isolated from nature.[26,27] For instance, the fredericamycin A is a natural spiro indan-1,3-dione presenting antitumor antibiotic activity.[28,29] Figure 1 shows the structures of indan-1,3-dione, some of its derivatives, and related properties.

We have been interested in the biological profile of indandiones. In this sense, we recently demonstrated the antiviral effect of 2-arylidene indan-1,3-diones.[30] We have also been involved in the search and development of new compounds that can be possible alternatives for cancer and leishmaniasis treatment.[31–46]

Within this scenario and with the aim of expanding the knowledge about the biological activities of indandione derivatives and their possible therapeutic potential, herein, we describe the evaluation of a series of 2-arylidene indandiones on *Leishmania amazonensis* as well as against two leukemia cancer cell lines. Besides, a four-dimensional quantitative structure–activity (4D-QSAR) analysis was applied to the indandione derivatives (and their activities) and the results are discussed.

2 | RESULTS AND DISCUSSION

2.1 | Preparation of 2-arylidene indan-1,3-diones

The compounds **1**, **3–16** (Table 1) investigated herein were prepared, in one step, from the zirconium-catalyzed Knoevenagel condensation reactions between indan-1,3-dione and different aromatic aldehydes.[30] The general reaction involved in the preparation of the compounds is shown in Scheme 1.

The indandione derivatives were prepared with yields ranging from 64% to 95%. It should be mentioned that compound **17** was obtained via demethylation of compound **13** with BBr_3.

2.2 | Cytotoxic and leishmanicidal activities of 2-arylidene indan-1,3-diones

Considering our interest in the discovery of alternative therapeutic options for the treatment of cancer and leishmaniases, once synthesized, the compounds **1**, **3–17** were subjected to biological assays to evaluate their leishmanicidal and cytotoxic activities against two lines of leukemia (Table 1).

To examine the cytotoxic effect of 2-arylidene indan-1,3-diones (**1**, **3–17**), we performed the MTT assay on the leukemia cell lines HL60 and Nalm6. As a general trend, the compounds showed moderate cytotoxic activity (Table 1). The inspection of IC_{50} values shows that the cytotoxic activity depends on the substitution pattern of the aromatic ring of the arylidene moiety. Considering the HL60 cell line, five of the 16 synthesized derivatives had IC_{50} values below 50 μmol/l (compounds **1**, **3**, **4**, **10**, and **12**). For the Nalm6, five presented IC_{50} values below 45 μmol/l (compounds **1**, **4**, **10**, **12**, and **15**). Considering these most active derivatives (**1**, **3**, **4**, **10**, **12**, and **15**), while compounds **1**, **3**, **4**, and **10** present as a common structural feature an arylidene moiety with one group at the *para*-position (**1** (–Cl); **3** (–Br); **4** (–NO_2); and **10** (–CN)), in compounds **12** and **15**, the aromatic ring of the arylidene portion has three groups. Another aspect to be noticed is that while derivatives **4** and **10** presented electron-withdrawing groups at the *para*-position in the arylidene moiety, compounds **12** and **15** displayed methoxy and hydroxyl groups, respectively, attached to the same position. Comparing the cytotoxic activity of **12** and **15**, the replacement of a methoxy group at the R^2 position (see Scheme 1) at the arylidene portion by a hydroxyl resulted in better activity for derivative **15**. Taking into

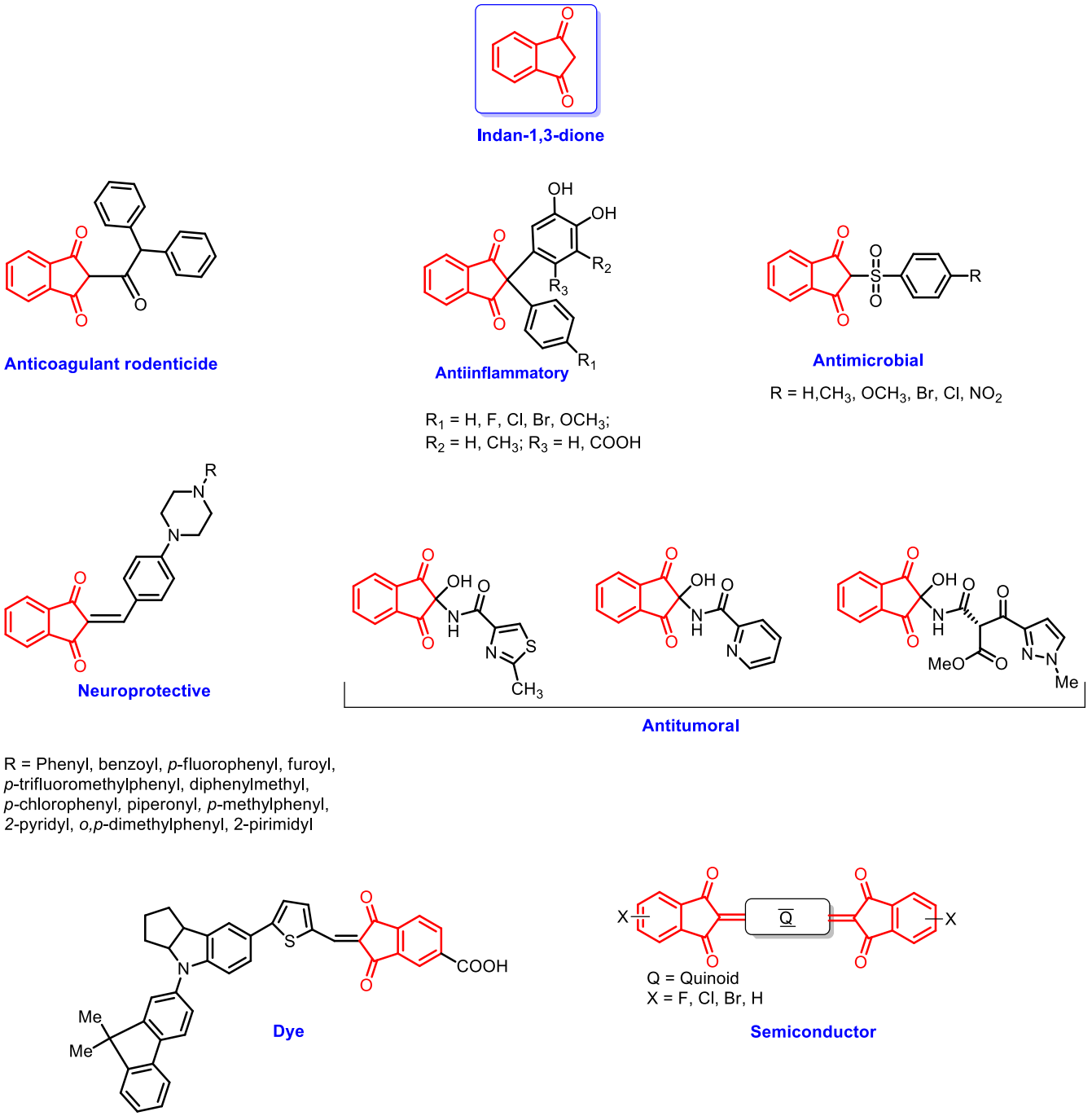

FIGURE 1 Indan-1,3-dione derivatives and related properties. In the structures of the derivatives, the indan-1,3-dione core is highlighted in red

account the compounds presenting methoxy and hydroxyl groups, the best substitution pattern in terms of improving cytotoxicity is related to the presence of three methoxy groups at R^1, R^2, and R^3 positions regarding the HL60 cell line and two methoxy groups at R^1 and R^3 and one hydroxy at R^2 for Nalm6. In terms of the halogenated compounds, the introduction of a fluorine at the R^2 position resulted in compounds with lower activity as compared to chlorine and bromine groups.

In the investigation performed by Pati et al.,[47] indandione derivatives presenting electron-withdrawing groups attached to the aromatic ring were prepared and evaluated on the leukemia cell line Molt4/C8, displaying IC_{50} values within 7–8 μmol/l. In the present investigation, the IC_{50} values of 2-arylidene derivatives **4** and **10**, which contain electron-withdrawing groups at the *para*-position of the arylidene portion, as evaluated against the Nalm6 leukemia cell line were around 30 μmol/l. Liu et al.[48] also biologically evaluated

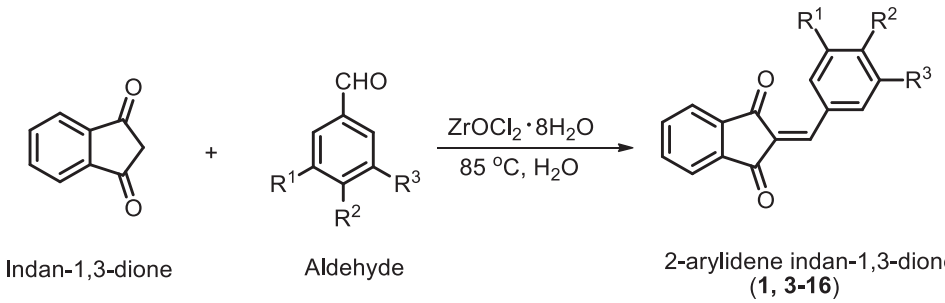

SCHEME 1 Zirconium-catalyzed Knoevenagel condensation involved in the preparation of 2-arylidene-indan-1,3-diones (**1**, **3–16**)

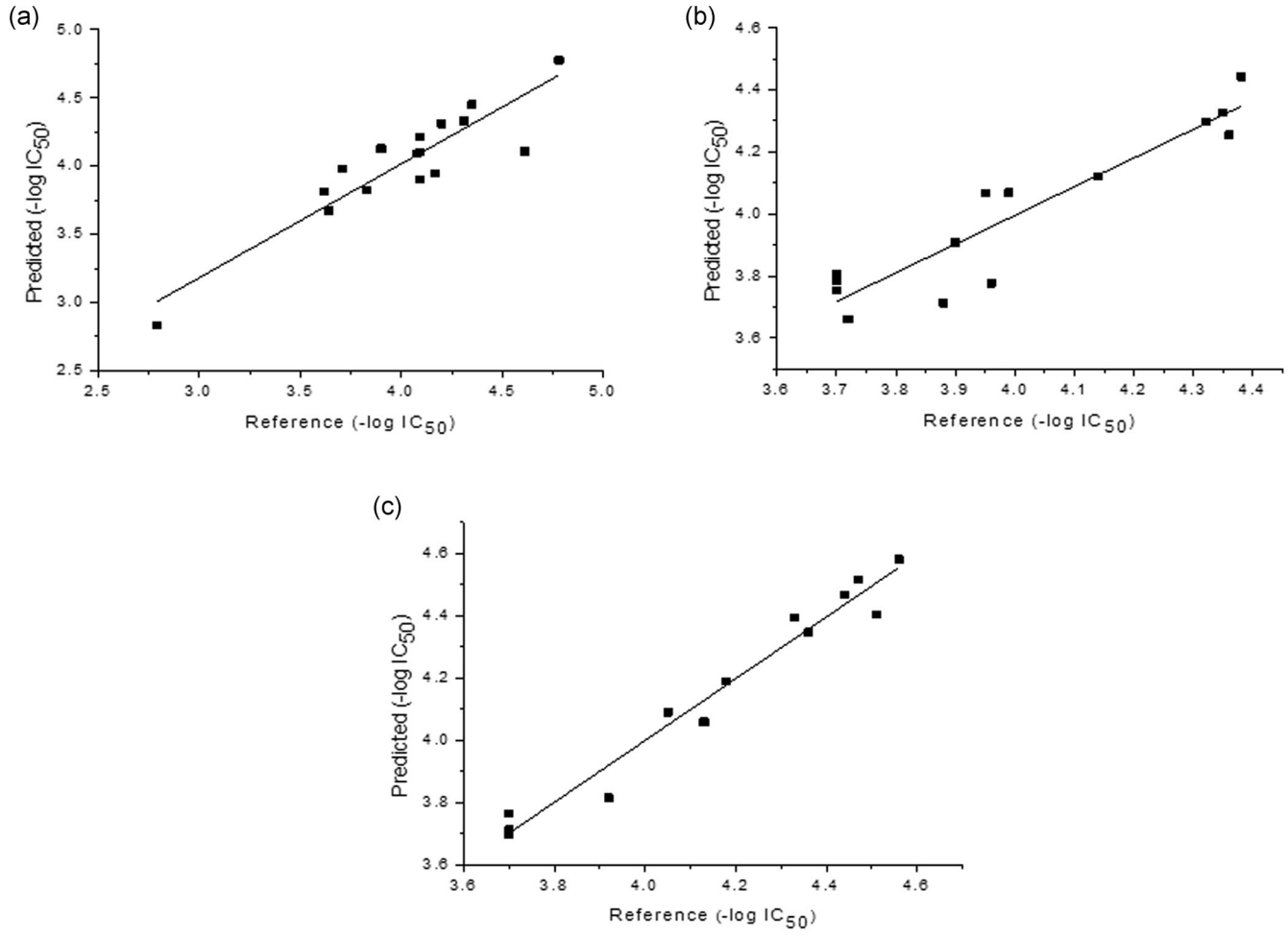

FIGURE 2 Plot of reference versus predicted values for 2-arylidene indan-1,3-diones tested against (a) *Leishmania amazonensis*, (b) HL60 leukemia cells, and (c) Nalm6 leukemia cells

indandione derivatives against the K562 leukemia cell line. The IC_{50} values described in the aforementioned study were lower than the IC_{50} described herein.

In terms of the effect of the compounds against the promastigote form of *L. amazonensis*, one of the etiologic agents of cutaneous leishmaniasis, it was found that, in general, the compounds presented IC_{50} values higher than 40 μmol/l. Exceptions to this trend are the most active derivatives **4** and **15**, which presented, respectively, IC_{50} values of 16.6 and 24.8 μmol/l. To the best of our knowledge, this is the first investigation of the leishmanicidal activity of 2-arylidene indan-1,3-diones.

Indandiones are a relatively new group of compounds that exhibit an interesting variety of biological activities. Unfortunately, little is known about the mechanisms of action of compounds derived from this group. However, different research groups that perform the synthesis and studies of the biological potential of indandiones

TABLE 1 Structures and effects of 2-arylidene indan-1,3-dione derivatives on promastigote forms of *Leishmania amazonensis* and on HL60 and Nalm6 leukemia cell lines

Compound[a]	Structure	IC_{50}[b] (μmol/l)/pIC_{50}[c]		
		L. amazonensis	HL60	Nalm6
1	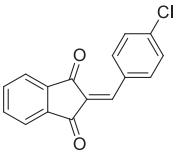	49.0 ± 0.2/4.31	47.88/4.32	42.76/4.36
3	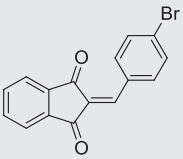	44.9 ± 0.2/4.35	45.08/4.35	46.58/4.33
4	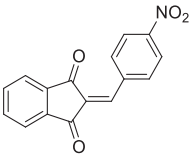	16.6 ± 0.2/4.78	41.99/4.38	33.92/4.47
5	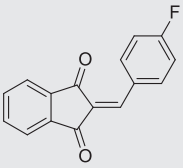	80.9 ± 0.2/4.09	71.85/4.14	66.76/4.18
6	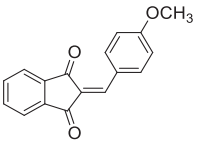	80.7 ± 0.1/4.09	111.60/3.95	88.90/4.05
7	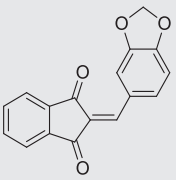	125.0 ± 0.1/3.9	126.90/3.9	>200/3.70
8	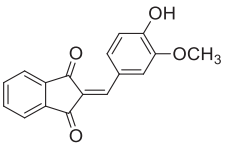	242.0 ± 0.3/3.62	>200/3.7	Inactive
9	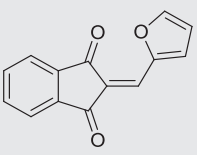	197.0 ± 0.1/3.71	189.30/3.72	>200/3.70
10	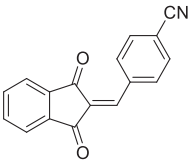	63.0 ± 0.1/4.2	45.10/4.35	27.30/4.56
11	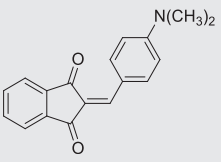	1618.0 ± 0.1/2.79	Inactive	Inactive

(Continues)

TABLE 1 (Continued)

Compound[a]	Structure	IC_{50}[b] (μmol/l)/pIC_{50}[c] *L. amazonensis*	HL60	Nalm6
12	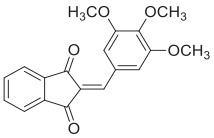	81.1 ± 0.1/4.09	43.97/4.36	36.51/4.44
13	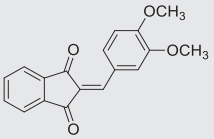	227.0 ± 0.2/3.64	>200/3.7	Inactive
14	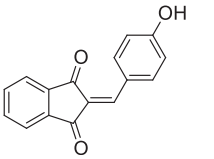	67.6 ± 0.2/4.17	103.30/3.99	>200/3.70
15	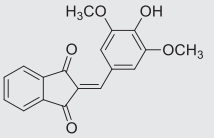	24.8 ± 0.3/4.61	>200/3.70	31.08/4.51
16	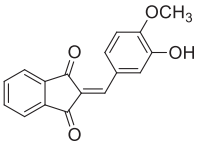	83.1 ± 0.1/4.08	133.00/3.88	73.89/4.13
17	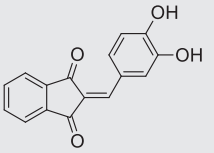	147.0 ± 0.2/3.83	110.20/3.96	120.70/3.92

[a]The compounds are numbered as previously reported.[16]

[b]The concentration of the compound required for 50% inhibition.

[c]pIC_{50} means $-\log IC_{50}$ (the pIC_{50} values were calculated by converting μmol/l into mol/l).

report that these derivatives showed promising antioxidant activity.[24,49] This activity is important, as studies attribute the antileukemia and leishmanicidal capacity of different substances to their antioxidative potential.[50–52] However, as already mentioned, little is known about the mechanisms of action of indandiones, and to better clarify the relationship between the activity and structure of the synthesized compounds investigated herein, QSAR models were performed and the results are presented in sequence.

2.3 | QSAR models for the studied activities of 2-arylidene indan-1,3-dione derivatives

The best regression models for 2-arylidene indan-1,3-dione derivatives tested against *L. amazonensis*, HL60, and Nalm6 leukemia cells (Figure 2) presented statistics (Table 2) that fulfill the minimal requirements for QSAR studies ($R^2 > 0.6$ and $Q^2LOO > 0.5$).[53,54] The selected molecular field descriptors are of both Coulomb (C) and Lennard-Jones (L) nature.

From the results obtained for 30–40 randomizations (y-randomization graphs a–c in Figures 3–5), one can conclude that the models are free of chance correlation. The intercepts for R^2 versus $R(\mathbf{y}_{rand}, \mathbf{y})$ and Q^2 versus $R(\mathbf{y}_{rand}, \mathbf{y})$ must be lower than 0.3 and 0.05, respectively, according to Eriksson et al.[55] The values found in graphs (a) and (b) of Figures 3–5 were 0.11; 0.15; and 0.13 for R^2 versus $R(\mathbf{y}_{rand}, \mathbf{y})$ and −1.16; −0.87; and −1.09 for Q^2 versus $R(\mathbf{y}_{rand}, \mathbf{y})$, respectively, for the three models. Besides, the Q^2 and R^2 values for randomized **y** (graphs c in Figures 3–5) were below or close to 0.00 and 0.40, respectively, confirming that the randomized models were of poor quality, as expected.

To assess the robustness of the models, LNO cross-validation (graphs d of Figures 3–5) was repeated 30–40 times, leaving one to five compounds out from the training sets one at a time for partial least-squares (PLS) models of the derivatives tested against

TABLE 2 Parameters for the evaluation and validation of the best PLS obtained models

Parameters	*Leishmania amazonensis*	HL60	Nalm6
Number of compounds	16	15	13
Number of factors	2	1	1
Descriptors[a]	–L3650, L3632, L2606, C541	L2600, L521, C540, L516, L663, C709, C2035	C1326, C2630, C2644, C2839, L2150 L2151, L2421, L2631, L3705
Total variance percent	54.18	57.17	57.09
R^{2}[b]	0.88	0.92	0.98
Q^{2}[c]	0.83	0.88	0.97
SEC[d]	0.17	0.08	0.05
SEV[e]	0.18	0.09	0.06
RE (%)[f]	2.40	1.48	0.85
Q^{2}_{LNO}[g]	0.81	0.86	0.96

Abbreviation: PLS, partial least squares.

[a]Molecular field descriptors of Coulomb (C) and Lennard-Jones (L) nature.

[b]Coefficient of multiple determination.

[c]Cross-validated correlation coefficient.

[d]Standard error of calibration.

[e]Standard error of cross-validation.

[f]Mean relative error.

[g]Five-fold cross-validated correlation coefficient for *L. amazonensis* and HL60 PLS models and four-fold cross-validated correlation coefficient for the Nalm6 PLS model.

L. amazonensis and HL60 leukemia cells. For the set tested against Nalm6 leukemia cells, there are a smaller number of compounds and, in this case, LNO cross-validation was performed, leaving one to four compounds out from the training set. For the three PLS models, the average Q^{2}_{LNO} values are close to the value of Q^{2}_{LOO}, and the standard deviations for each *N* value are small, indicating that the QSAR models are robust.

The predictive ability of the models can be assessed by the results obtained for the five- or four-fold cross-validation (graphs d in Figures 3–5), once the total sets of the studied compounds are small (16, 15, and 13 compounds evaluated against *L. amazonensis*, HL60, and Nalm6 leukemia cells, respectively) to select external test sets. The residues and calculated relative error (Table S1), the respective mean relative errors (RE), and the Q^{2}_{LNO} ($N = 5$ or $N = 4$) values in Table 2 indicated that the final models can be used for the prediction of new bioactive compounds.

2.4 | Descriptor discussion for regression models

2.4.1 | Leishmanicidal activity

According to the autoscaled regression coefficients signals in Equation (1), the leishmanicidal activity is positively correlated to Coulomb and Lennard-Jones descriptors C541, L2606, and L3632, and negatively correlated to the L3650 descriptor. This means that pIC_{50} increases when the Coulomb and van der Waals interactions (described by C541, L2606, and L3632) increase, and decreases when L3650 increases.

$$pIC_{50} = 0.34C541 + 0.26L2606 + 0.19L3632 - 0.50L3650 \quad (1)$$

To evaluate the consistency of the model, the signals of the coefficients for the correlation between pIC_{50} and the descriptors were also investigated.[56] From the coincidence of the signals for the regression coefficients in the model (Equation 1) and the signals of correlation coefficients between each respective descriptor and pIC_{50} (+0.67 C541; +0.68 L2606; +0.66 L3632; −0.71 L3650), this model proved to be self-consistent.

The position of the field descriptors used to build the PLS model, considering compound **15**, which is one of the most active and bulky derivatives, can be visualized in Figure 6, where − and + are the signals of the regression coefficients in the model. The negative Lennard-Jones (L) descriptor L3650 is located close to the R^{2} substituent, meaning that great van der Waals interactions on this position are unfavorable for leishmanicidal activity. On the other hand, two positive L descriptors are located near R^{3} (Figure 9), suggesting that bulky substituents attached to this position favor the biological activity. Comparing compounds **12** and **15** (Figure 9 and Table 1), the activity reduced drastically

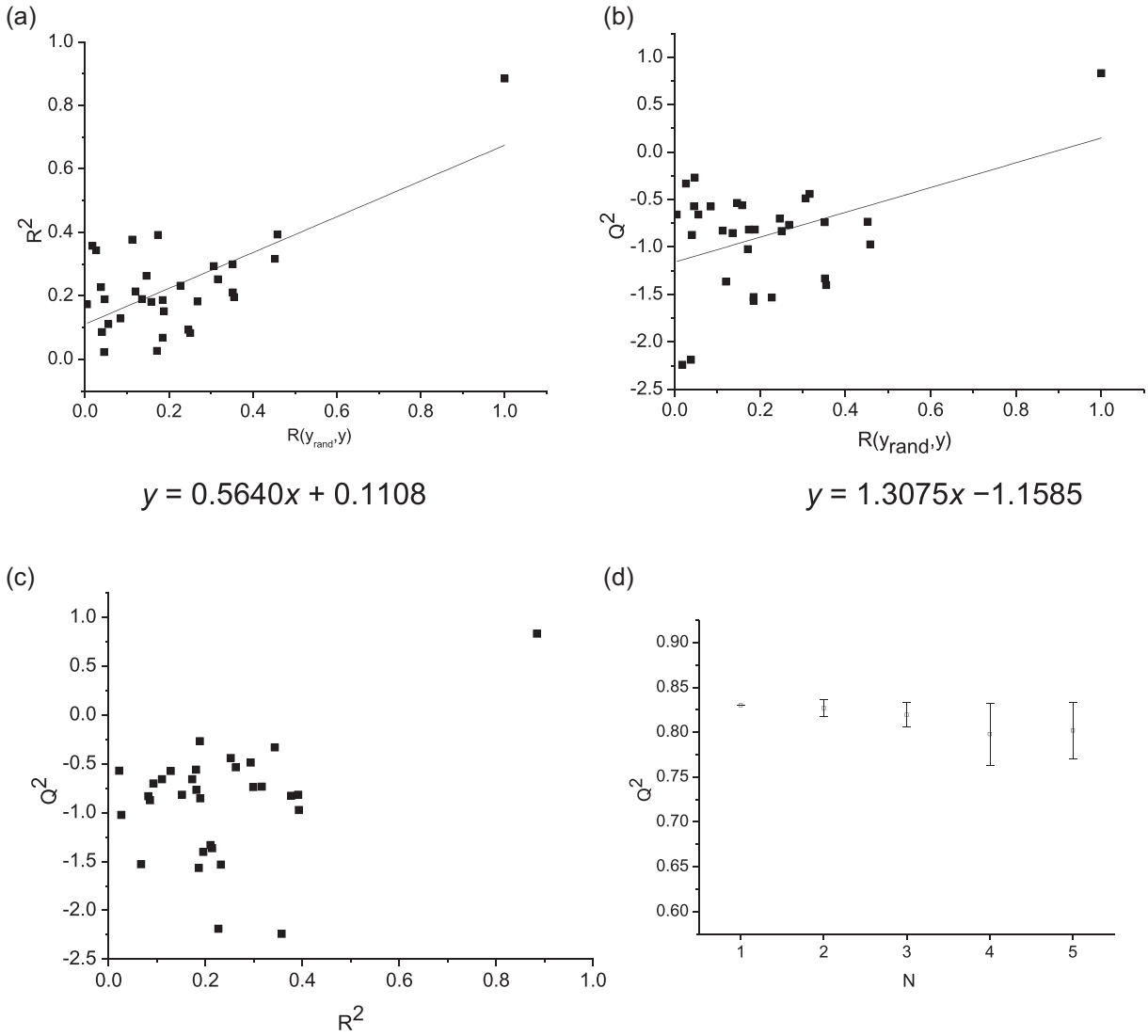

FIGURE 3 Plots of the y-randomization test (30 repetitions) for the partial least-squares model of 2-arylidene indan-1,3-dione derivatives tested against *Leishmania amazonensis*, where $R(y_{rand}, y)$ means R ($pIC_{50randomized}$, pIC_{50}). (a) R^2 versus $R(y_{rand}, y)$; (b) Q^2 versus $R(y_{rand}, y)$; and (c) Q^2 versus R^2, where Q^2 is the coefficient of determination for LOO cross-validation. (d) LNO cross-validation (N = 1–5) for 30 repetitions

when the substituent in R^2 was changed from hydroxyl in **15** (pIC_{50} = 4.61) to the bulkier group, $-OCH_3$ in **12** (pIC_{50} = 4.09).

From Equation (1) and the location of the descriptors in Figure 6, polar groups at position R^2 do not seem to be favorable for the leishmanicidal activity, in agreement with the experimental results shown in Table 1. Considering the substituents at R^2 (Table 1) for compounds **5** (–F), **14** (–OH), **1** (–Cl), and **3** (–Br), and the respective values of pIC_{50} (4.09; 4.17; 4.31; 4.35), one can see that the activity decreases with the increase in electronegativity of the substituents in this position.

The PLS regression model suggests that the interaction between the ring where substitutions were made and the receptor occurs mainly by van der Waals interactions. Thus, the activity would be favored by large nonpolar substituents at position R^3 and small nonpolar substituents at R^2.

Also, the positive Coulomb descriptor close to the carbonyl groups confirms the importance of these groups to the biological activity of 2-arylidene indan-1,3-dione derivatives, which is corroborated by the literature.[47,57,58]

It is known that the bioactivity of α,β-unsaturated ketones is related to the conjugated double bond with the carbonyl functionality (–CO–CH═CH–), as removal of the enone group in chalcones, for example, renders them inactive.[57,58] This α,β-unsaturated ketone fragment is also present in the series of 2-arylidene-1,3-indandiones under investigation. Pati et al.[47] performed molecular modifications in a series of 2-arylidene-1-indanones previously evaluated for cytotoxic properties, generating a new series of 2-arylidene-1,3-indandiones and another of chalcones. These modifications were made to find explanations for the variation in bioactivities. The authors found that cytotoxicity and the fractional positive charge on the olefinic carbon atom were increased by

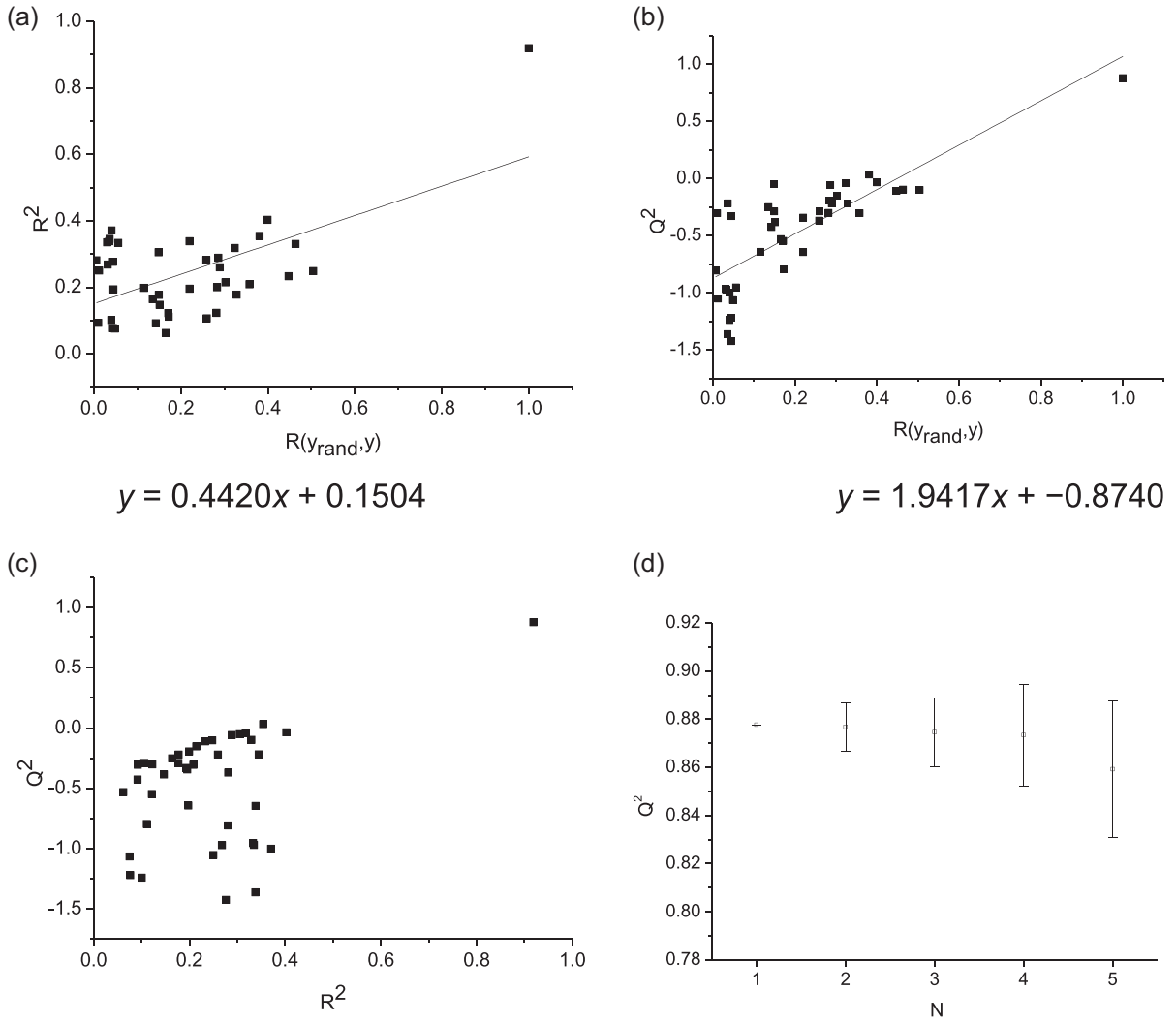

FIGURE 4 Plots of the y-randomization test (40 repetitions) for the partial least-squares model of 2-arylidene indan-1,3-dione derivatives tested against HL60 leukemia cells, where $R(y_{rand}, y)$ means R ($pIC_{50randomized}$, pIC_{50}). (a) R^2 versus $R(y_{rand}, y)$; (b) Q^2 versus $R(y_{rand}, y)$; and (c) Q^2 versus R^2, where Q^2 is the coefficient of determination for LOO cross-validation. (d) LNO cross-validation (N = 1–5) for 40 repetitions

placing the additional electron-attracting oxygen atom into the indane scaffold,[47] reinforcing the importance of the carbonyl groups for the bioactivity of these compounds.

The results of the 4D-QSAR analysis provided some insights into the mode of interaction with the receptor. However, it was not possible to fully explain the variations in activity with the substitutions at positions R^1 to R^3. Although the regression model works for the majority of this series of compounds, some of them do not fit the presented analysis, as the most active compound **4**, suggesting the necessity of further investigations.

2.4.2 | Cytotoxic activity against the Nalm6 cell line

As the first step to this analysis, the consistency of the model presented in Equation (2) was evaluated by comparison of the autoscaled regression coefficients signals (Equation 2) and the signals of correlation coefficients[56] between each respective descriptor and pIC_{50} (+0.63 C1326; −0.71 C2630; −0.71 C2644; −0.80 C2839; +0.72 L2150; +0.79 L2151; +0.79 L2421; +0.83 L2631; −0.73 L3705). The coincidence of the signals proved that this model is self-consistent.

$$pIC_{50} = 0.12C1326 - 0.14C2630 - 0.14C2644 - 0.16C2839 + 0.14L2150 + 0.15L2151 + 0.15L2421 + 0.16L2631 - 0.14L3705 \quad (2)$$

The location of the field descriptors selected to build the PLS model, around the bulky and active compound **15**, can be visualized in Figure 7. From Equation (2), the biological activity against Nalm6 leukemia cells is positively correlated with the Coulomb descriptor C1326, located close to one of the carbonyl groups that are crucial for the bioactivity of this class of compounds.[57,58] Lennard-Jones descriptors, positively correlated with pIC_{50}, are located close to position R^1 of the compounds

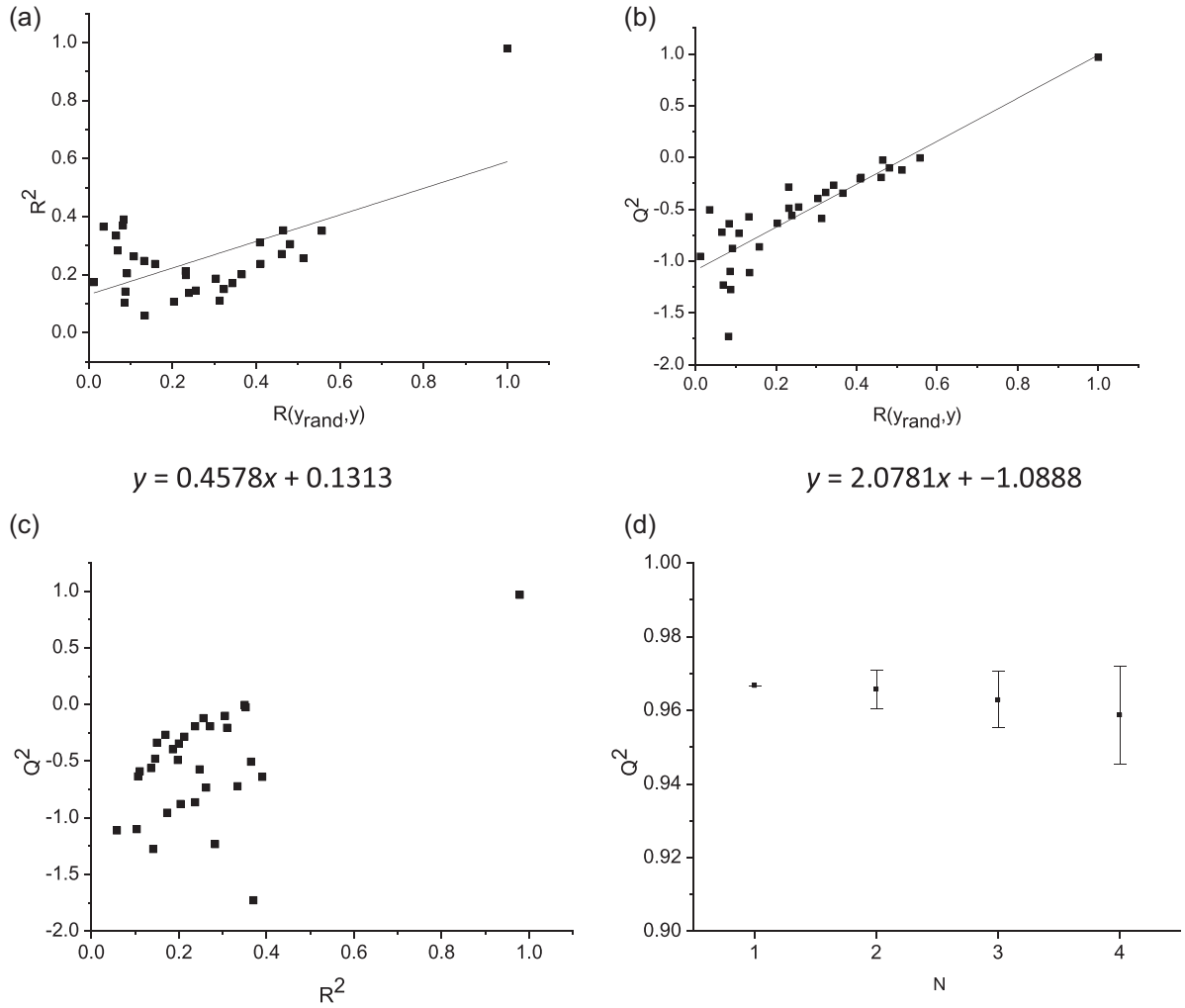

FIGURE 5 Plots of the y-randomization test (30 repetitions) for the partial least-squares model of 2-arylidene indan-1,3-dione derivatives tested against Nalm6 leukemia cells, where $R(y_{rand}, y)$ means R ($pIC_{50randomized}$, pIC_{50}). (a) R^2 versus $R(y_{rand}, y)$; (b) Q^2 versus $R(y_{rand}, y)$; and (c) Q^2 versus R^2, where Q^2 is the coefficient of determination for LOO cross-validation. (d) LNO cross-validation (N = 1–4) for 30 repetitions

(Figures 7 and 9), indicating that the biological activity is favored by van der Waals interactions in that region, so that bulky nonpolar substituents in R^1 tend to increase pIC_{50}. Besides this, the presence of three negative Coulomb descriptors between R^1 and R^2 positions is indicative that polar substituents in these positions are unfavorable to biological activity, corroborating the assumption that pIC_{50} tends to increase with bulky and nonpolar substituents in R^1.

The negative Lennard-Jones descriptor (−L3705) is located close to substituents R^2 and R^3, where bulky groups would be unfavorable for the considered biological activity. From these results, one can assume that the interaction of the compounds with the receptor occurs mainly by substituents in the R^1 position and by the carbonyl group located close to the R^1 position. The model also indicated that the biological activity under investigation is favored by bulky and nonpolar substituents in the R1 position, which explains the activity of the majority of the studied compounds. However, the model could not explain the high activity of compounds **4** and **10**, indicating that other factors related to bioactivity, besides those found in this analysis, need to be explored.

2.4.3 | Cytotoxicity against the HL60 cell line

The regression model in Equation (3) is self-consistent, as can be observed by the coincidence of the autoscaled regression coefficients signals (Equation 3) and the signals of correlation coefficients[56] between each respective descriptor and pIC_{50} (+0.83 C540; +0.85 C709; +0.68 C2035; −0.72 L516; −0.71 L521; −0.62 L663; +0.63 L2600), as explained before.

$$pIC_{50} = 0.21C540 + 0.21C709 + 0.17C2035 - 0.18L516 - 0.17L521 - 0.16L663 + 0.16L2600 \quad (3)$$

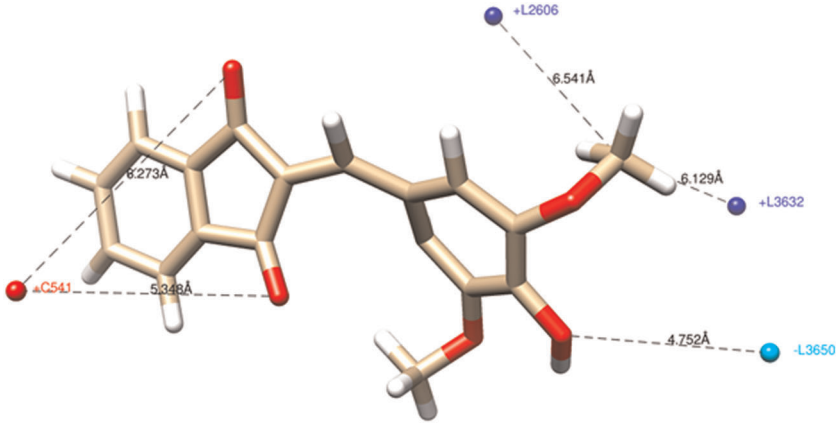

FIGURE 6 Compound **15** and 4D descriptors used to build the partial least-squares models for 2-arylidene indan-1,3-dione derivatives tested against *Leishmania amazonensis*. C and L are the Coulomb and Lennard-Jones descriptors, and − and + are the signals of the regression coefficients in the model

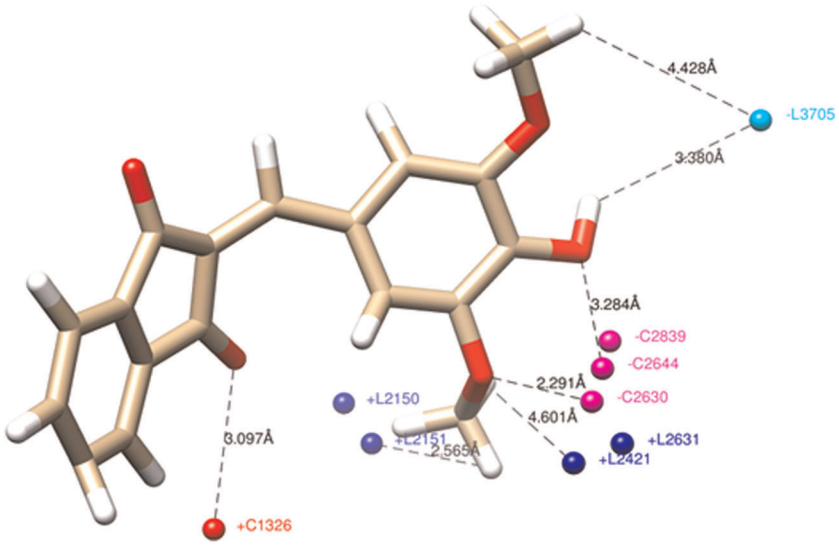

FIGURE 7 Compound **15** and 4D descriptors used to build the partial least-squares models for 2-arylidene indan-1,3-dione derivatives tested against Nalm6 leukemia cells. C and L indicate the Coulomb and Lennard-Jones descriptors, and − and + are the signals of the regression coefficients in the model

The location of the field descriptors (Figure 8) around compounds **12** (active; Table 1) and **13** (very low activity; Table 1) suggests a mode of interaction with the receptor similar to that presented for the analysis of the series tested against the Nalm6 leukemia cells. One can observe a positive Lennard-Jones descriptor close to the R^1 position, indicating that pIC_{50} increases with great van der Waals interaction in this region. The positive Coulomb descriptors close to the carbonyl moieties provide evidence, again, of the importance of these groups for the bioactivity of this class of compounds and suggest that this region could also be involved in the interactions with the receptor. The presence of negative Lennard-Jones descriptors near the ring without substituents means that bulky and nonpolar groups in this region of the molecules induce a decrease in the activity.

These results suggest that the interaction with the receptor in HL60 leukemia cells may occur mainly by bulky and nonpolar groups located in the R^1 position and by the carbonyl moieties present in the indan-1,3-dione structure. It is interesting to notice that at least one positive Coulomb descriptor is present in the vicinities of carbonyl groups in the models discussed here, but for the activity against HL60 leukemia cells, there are three Coulomb descriptors close to carbonyl moieties, positively correlated with pIC_{50}. Previous 4D-QSAR analysis[59] of a series of 1,4-naphthoquinones tested against HL60 leukemia cells also presented positive Coulomb descriptors located close to the carbonyl groups (quinone oxygens) involved in the production of radical anions ($O_2^{-\bullet}$). Quinones can generate reactive oxygen species (ROS) through the activation by the cytochrome P450 and P450 reductase enzymes acting as anticancer agents.[60] Comparing the results of both 4D-QSAR analysis for compounds tested against HL60 leukemia cells, one can suggest that ROS could also be generated by the indan-1,3-dione moiety.

3 | CONCLUSIONS

The present investigation contributed toward broadening the pharmacological profile of indan-1,3-dione derivatives. Sixteen compounds prepared from indan-1,3-dione and bearing arylidene fragments had two biological activities that were evaluated. For the first time, the leishmanicidal effect of 2-arylidene indan-1,3-diones on *Leishmania amazonensis*, one of the most important

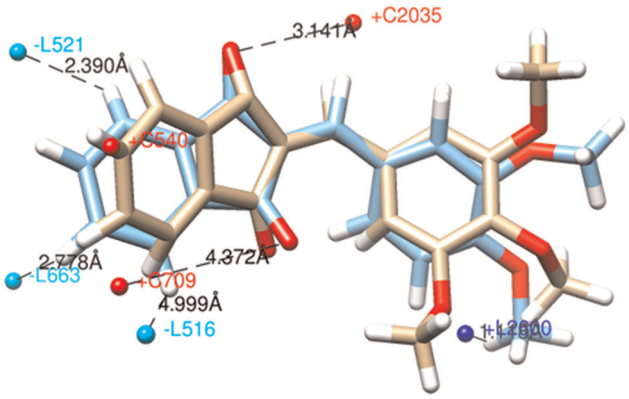

FIGURE 8 Superimposed compounds **12** (active) and **13** (very low activity), and 4D descriptors used to build the partial least-squares models for 2-arylidene indan-1,3-dione derivatives tested against HL60 leukemia cells. C and L indicate the Coulomb and Lennard-Jones descriptors, and − and + are the signals of the regression coefficients in the model

etiological agents of cutaneous leishmaniasis, was demonstrated. It was possible to conclude that the leishmanicidal potency of the derivatives depends on the substitution pattern of the aromatic ring of the arylidene moiety. The most active derivative displayed an IC_{50} value of around 15 µmol/l. The cytotoxic effect of the 2-arylidene indan-1,3-dione derivatives was also assessed against HL60 and Nalm6 leukemia cell lines, and the most active compounds presented IC_{50} approximately equal to 30 µmol/l. As noticed with the leishmanicidal activity evaluation, the cytotoxicity is dependent on the substitution pattern of the arylidene moiety. Considering that the cytotoxicity profile of indan-1,3-dione derivatives has been little explored, the results described in this investigation contribute toward increasing the knowledge in this field. A 4D-QSAR analysis was performed considering the three investigated biological activities. It was found that the carbonyl groups of indan-1,3-diones are very important in terms of the evaluated bioactivities. With the field descriptors selected by the regression models, it was possible to gain some insights into the mode of action of this series for each investigated biological activity. The activity of the 2-arylidene indan-1,3-dione derivatives against *L. amazonensis* is favored by bulky nonpolar substituents at the R^3 position, while the cytotoxic effects of the compounds against HL60 and Nalm6 leukemic cells are favored by the same type of substituents, but at the R^1 position. Bulky nonpolar groups in the R^2 position do not favor the activity against *L. amazonensis* and on Nalm6 leukemic cells. The positive Coulomb descriptors close to the carbonyl moieties suggest that these groups can participate in the interactions with the receptor. It is believed that the results found in the present study open new possibilities for the design of more potent indandione derivatives and may result in the discovery of new pharmaceuticals that can be helpful in the treatment of leishmaniasis and cancer. Further investigations in this regard are underway in our group.

4 | EXPERIMENTAL

4.1 | Preparation of indan-1,3-dione derivatives

The compounds investigated herein, **1**, **3–17** (Table 1) (the InChI codes are listed in the Supporting Information, together with biological activity data), were prepared as previously described.[30]

4.2 | Antileishmanial activity of 2-arylidene indan-1,3-diones

Promastigotes of *L. amazonensis* (WHOM/BR/75/Josefa) were cultured in M199 medium, supplemented with 50 IU/ml of penicillin, 50 µg/ml of streptomycin, 10% (v/v) of heat-inactivated fetal calf serum, and 2% (v/v) of human urine at 26°C. For evaluation of the antipromastigote activity, promastigotes of *L. amazonensis* were plated in triplicate at 5×10^5 parasites/ml with varying concentrations of the tested compound (0, 0.1, 1, 10, and 100 µmol/l) in a final volume of 200 µl of medium M199 containing 5% (v/v) of HIFCS and 1% (v/v) of dimethyl sulfoxide (DMSO). After 72 h of incubation, parasite viability was assessed by adding resazurin (50 µmol/l) for an additional 3 h. The fluorescence was quantified (excitation λ = 560 nm; emission λ = 590 nm), and the data obtained from three experiments were expressed as the mean ± standard error of the mean (mean ± SEM). The half-maximal inhibitory concentration (IC_{50}) was determined by logarithmic nonlinear regression analysis using GraphPrism software (version 5, GraphPad).

4.3 | Cytotoxicity evaluation of 2-arylidene indan-1,3-diones

Human leukemia cell lines HL60 (acute myelogenous leukemia) and Nalm6 (acute lymphoblastic leukemia) were kindly provided by Dr. Jose Andrés Yunes (Centro Infantil Boldrini, Campinas, São Paulo, Brazil). Cell lines were grown in Roswell Park Memorial Institute (RPMI)-1640 medium (Sigma) supplemented with 10% (v/v) fetal bovine serum (FBS; LGC Biotecnologia), 100 µg/ml of streptomycin, and 100 units/ml of penicillin (Sigma) at pH 7.2 and 37°C under a 5% CO_2 atmosphere. Cell viability was evaluated using the MTT (3-(4,5-dimethylthiazol-2-yl)-2,5-diphenyltetrazolium bromide) method.[61] HL60 and Nalm6 cells were seeded onto 96-well plates at a concentration of 1×10^4 cells/well. Each well contained 100 µl of complete RPMI medium and 100 µl of each compound solution at different concentrations (200, 150, 100, 50, 25, 12.5, and 6.25 µmol/L). The cells were incubated at 37°C under 5% of CO_2 for 48 h. All the compounds **1** and **3–17** were diluted in RPMI medium with 10% FBS plus DMSO (0.4% v/v) (Sigma). After 48 h of culture, MTT (5 mg/ml; Sigma) was added to each well and incubated for 4 h at 37 °C. The MTT solution was then removed and DMSO (100 µl/well) was added to solubilize the formazan. After 20 min at 37°C, absorbance was measured at 540 nm in a microplate reader

(SpectraMax M5, Molecular Devices). Analyses were carried out in triplicate and the results were normalized considering the cells treated with only DMSO (0.4% v/v). The half-maximal inhibitory concentration (IC_{50}) values were determined using GraphPadPrism version 6.1. Compounds presenting an inhibitory effect lower than 10% at 200 µmol/l were considered inactive.

4.4 | Geometry optimization of 2-arylidene indan-1,3-diones

In the absence of the crystallized binder–receptor complex, the three-dimensional geometry of the 2-arylidene indan-1,3-dione derivatives (Table 1) was prepared based on the crystallographic data from compounds **1** (2-(4-chlorobenzylidene)-1*H*-indene-1,3(2*H*)-dione) and **15** (2-(4-hydroxy-3,5-dimethoxybenzylidene)-1*H*-indene-1,3(2*H*)-dione), found in the Cambridge Structural Database (CSD),[62] entries XICLIH (https://www.ccdc.cam.ac.uk/structures/search?id=doi:10.5517/ccdc.csd.cc1lsgc6%26sid=DataCite) and XICLED (https://www.ccdc.cam.ac.uk/structures/search?id=doi:10.5517/ccdc.csd.cc1lsgb5%26sid=DataCite), respectively. The geometries of these two compounds were, posteriorly, optimized by the DFT/B3LYP method, with the def2-TZVPP basis set,[63] using Gaussian 9.0.[64] This triple zeta valence basis set is a high-quality Gaussian basis set optimized for atoms from H to Rn and was chosen mainly due to the presence of bromine in one of the studied compounds (Table 1).

Starting from the optimized geometries of compounds **1** and **15**, the three-dimensional geometries of all other derivatives were constructed using GaussView 3.0 software,[65] by changing or adding the substituents R^1, R^2, and R^3 (Figure 9 and Table 1). The conformational search of each substituent was performed using the PM3 semiempirical method using the keyword *scan* from Gaussian 9.0.[64] To determine the local minima conformations, the axes *a*, *b*, and *c* (and *d* for compound **9**) depicted in Figure 9 were rotated with a 15° increment. The conformational analysis involves the search for the biologically active conformation, which is not necessarily the most stable conformation (global minimum). Flexible molecules can adopt a large number of stable conformations that can better fit the target than the global minimum. Sometimes, the global minimum is stabilized by intramolecular interactions, which may not be favorable to a binder–receptor interaction. Based on this argument, stable conformations visually presenting few intramolecular interactions were chosen. Then, the selected local minimum of each compound was optimized using the DFT/B3LYP method as described above.

4.5 | 4D-QSAR analysis

The methodology chosen for the QSAR analysis was the LQTA-QSAR approach[66] that is based on the generation of a conformational ensemble profile (CEP), instead of considering a single conformation. The CEPs were generated through molecular dynamics (MD) simulation for each compound, which incorporates conformational freedom into the development of 3D-QSAR models. This conformational freedom would be the fourth dimension.

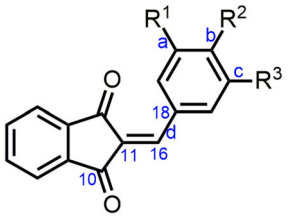

FIGURE 9 Basic structure of 2-arylidene indan-1,3-dione derivatives. The numbering of the atoms indicated in this figure is the same as that from the GaussView program

MD simulations, performed using the GROMACS-4.6.5[67] computational package, were applied to the optimized molecular geometries using LQTA-QSAR software.[66] An explicit aqueous medium was considered. Each compound was placed in a cubic box with a minimum distance of 10 Å from the molecule to the edge of the box, which was then filled with water molecules. Atomic positions were optimized using the steepest descent and conjugate gradient algorithm with 50 N of maximum force applied to the atoms, as the convergence criterion. The system was heated following the scheme of 50, 100, 200, and 350 K for a 10 ps simulation time performed in a 2-fs step size. Then, the system was cooled to 300 K and simulated for 500 ps. The conformations obtained from each compound were recorded every 10 ps for 500 ps and then they were organized in *. gro files for the construction of the CEP.

To build the CEP with all conformations of all compounds (Figure S1), the resulting conformations from MD simulations were aligned by atoms 10, 11, 16, and 18 (Figure 9). After that, a virtual cubic grid was built, large enough to contain the CEP of all molecules, whose dimensions were 17 × 14 × 13 Å. Then, the LQTAgrid module from the LQTA-QSAR program[66] was used to calculate the field descriptors, selecting as a probe the fragment NH_3^+ that mimics the amino-terminal portion of peptides. The interaction energies were calculated using the atomic charges from electrostatic potentials (ChelpG), obtained with Gaussian 9.0 during the optimization of the geometries. Each point of the virtual grid, with 1 Å resolution, was explored by the probe, and 7560 descriptors were generated. The field descriptors are the contributions of electrostatic and van der Waals energies (Coulomb and Lennard-Jones potentials) obtained by the interaction between the probe NH_3^+ and each point of the grid, according to Equations (4) and (5), respectively.

$$E_C = \frac{1}{n}\sum_{i=1}^{i}\frac{q_i \quad q_j}{4\pi\varepsilon_0 r_{ij}}, \tag{4}$$

$$E_{LJ} = \frac{1}{n}\sum_{i=1}^{i}\left[\frac{C_{ij}^{12}}{r_{ij}^{12}} - \frac{C_{ij}^{6}}{r_{ij}^{6}}\right] \quad \rightarrow \quad \begin{matrix} C_{ij}^{12} = \left(C_{ii}^{12} \times C_{jj}^{12}\right)^{1/2} \\ C_{ij}^{6} = \left(C_{ii}^{6} \times C_{jj}^{6}\right)^{1/2}. \end{matrix} \tag{5}$$

In Equations (4) and (5), q_i is the charge of the ith atom from CEP, q_j is the charge of the probe, ε_0 is the vacuum permittivity, $C_{ii}^{(12)}$, $C_{ii}^{(6)}$, $C_{jj}^{(12)}$, and $C_{jj}^{(6)}$ are parameters adapted from the ffG43a1 Gromos force field[66] for atoms in CEP and the probe, respectively, n indicates the number of conformations aligned in CEP, and r_{ij} is the distance between the j probe and the ith atom of CEP.

4.6 | Descriptor extraction

As the first step in descriptor extraction, those with variance below 0.02 were excluded, as indicated by Kubinyi.[68] The resulting descriptors were filtered, in the second step, using a correlation coefficient cut-off, where those presenting a Pearson correlation coefficient with **y** (biological activity) lower than 0.3 were eliminated. The next and last step was to eliminate descriptors with poor distribution profiles concerning **y** utilizing the digital filter Comparative Distribution Detection Algorithm (CDDA). According to Barbosa and Ferreira,[69] CDDA provides a way to quantify how similarly distributed **y** and a given descriptor are, enabling the removal of those not well distributed. At the end of these procedures, the field descriptors were reduced from 7560 to 546 for the leishmanicidal activity, from which 537 were Coulomb (C) and nine were Lennard-Jones (L) descriptors. For the activities against HL60 and Nalm6 leukemia cells, the numbers of descriptors were reduced to 720 (644 C and 76 L) and 139 (135 C and 4 L), respectively.

4.7 | PLS regression

The remaining descriptors were organized in matrices **X**, one for each subset of compounds (Table 1), and correlated with the corresponding $-\log IC_{50}$ values arranged in column vectors **y**, using QSAR modeling software.[70] The Ordered Predictors Selection (OPS) Algorithm[71] was applied to the autoscaled data, for a further selection of descriptors. The aim of this method is to obtain a vector that contains information about the location of the best variables for prediction. The columns of matrix **X** are reordered such that the most important descriptors are placed in the first columns. Then, PLS regressions are built successively to find the best model. The number of factors is determined using the leave-one-out (LOO) cross-validation method. In the end, only four, seven, and five descriptors for leishmanicidal, HL60 cytotoxic activity, and Nalm6 cytotoxicity, respectively, were selected.

In this study, the applicability domain is defined by the leverage and the studentized residuals. The presence of outliers was analyzed by observing the plot of leverage versus studentized residuals (Figure S2). For the PLS model of the derivatives tested against *L. amazonensis*, compound **15** (Figure S2a) presented a studentized residual somewhat beyond the critical value of 2.0,[53,54] while compounds **4** and **11** presented large leverages. For PLS models of the derivatives tested against HL60 and Nalm6 leukemia cells (Figure S2b,c), compounds **4**, **9**, and **14** presented somewhat large values of leverage. Nevertheless, no compounds were removed from the data sets, which contain a small number of compounds.

The quality of the final regression models was assessed by analyzing the coefficient of multiple determination (R^2), the standard error of calibration (*SEC*), the cross-validated correlation coefficient (Q^2), and the standard error of cross-validation (*SEV*).

The *y*-randomization test[53,54] was applied to investigate the presence of chance correlation between the dependent variable and descriptors, that is, descriptors that are statistically well correlated to **y**, although in reality not related to the problem under investigation. For this test, only the vector **y** is randomized ($\mathbf{y}_{rand}$), while the matrix **X** is left untouched. New parallel models were developed with the values of the original descriptors kept untouched and the values of the dependent variable, **y**, permuted between the compounds. In this study, 30–40 randomization runs were carried out. It is expected that the statistical parameters from the randomized models (Q^2_{yrand} and R^2_{yrand}) should be significantly lower than those obtained for nonrandomized data (Q^2_{LOO} and R^2). Another approach to judge whether the real model is characterized by chance correlation is based on the absolute value of the Pearson correlation coefficient $R(\mathbf{y},\mathbf{y}_{rand})$, between the original vector **y** and the randomized vector $\mathbf{y}_{rand}$. Two **y** randomization plots, $R(\mathbf{y},\mathbf{y}_{rand})$ versus Q^2 and $R(\mathbf{y},\mathbf{y}_{rand})$ versus R^2, were drawn for all randomized and real models. Two linear equations of $R(\mathbf{y},\mathbf{y}_{rand})$ versus Q^2 and $R(\mathbf{y},\mathbf{y}_{rand})$ versus R^2 were obtained for each model. It has been recommended that for a model free of chance correlation, the intercepts are $a_Q < 0.05$ and $a_R < 0.3$.[64]

To test the robustness of the model, leave-*N*-out (LNO) cross-validation was performed. In this test, **X** and **y** are simultaneously randomized and divided into blocks of *N* samples. Then, each block is excluded once and a new model is built on the reduced data set. LNO was repeated 30 times for analysis against leishmaniasis and 40 times for analyses against both types of leukemia cells, for *N* varying from 1 to 5 for leishmaniasis and the HL60 cell line, and from 1 to 3 for Nalm6 leukemia cells; the average Q^2_{LNO}, with its standard deviation, was calculated for each value of *N*. The critical *N* is the maximum value for which Q^2_{LNO} is still stable and high. For a good model, the average Q^2_{LNO} should remain close to Q^2_{LOO}, with small variations at all values for *N* up to the critical *N*. From our experience, 2 SD should not be greater than 0.1 ($Q^2_{LOO} \pm 0.05$) for $N = 2, 3$, and so forth, including the critical value of *N*.

ACKNOWLEDGMENTS

We are grateful to CNPq, CAPES, FAPEMIG, and FAPESP for financial support.

CONFLICT OF INTERESTS

The authors declare that there are no conflicts of interest.

ORCID

Róbson R. Teixeira http://orcid.org/0000-0003-3181-1108

REFERENCES

[1] S. Burza, S. L. Croft, M. Boelaert, *Lancet* **2018**, *392*, 951.
[2] J. Alvar, I. D. Velez, C. Bern, M. Herrero, P. Desjeux, J. Cano, J. Jannin, M. den Boer, *PLoS One* **2012**, *7*, e35671.
[3] WHO. *Leishmaniasis Fact Sheet No. 375*. WHO, Geneva, Switzerland **2015**. http://www.who.int/mediacentre/factsheets/fs375/en/ (accessed: December 2020).
[4] A. K. Haldar, P. Sen, S. Roy, *Mol. Biol. Int.* **2011**, *2011*, 571242.
[5] F. Frézard, C. Demicheli, R. R. Ribeiro, *Molecules* **2009**, *14*, 2317.
[6] B. S. McGwire, A. R. Satoskar, *QJM* **2014**, *107*, 7.
[7] S. L. Croft, S. Sundar, A. H. Fairlamb, *Clin. Microbiol. Rev.* **2006**, *19*, 111.
[8] S. L. Croft, G. H. Coombs, *Trends Parasitol.* **2003**, *19*, 502.
[9] M. Ouellette, J. Drummelsmith, B. Papadopoulou, *Drug Resist. Updates* **2004**, *7*, 257.
[10] L. Monzote, *Open Antimicrob. Agents J.* **2009**, *1*, 9.
[11] S. H. Hassanpour, M. Dehghani, *J. Cancer Res. Pract.* **2017**, *4*, 127.
[12] C. B. Blackadar, *World J. Clin. Oncol.* **2016**, *7*, 54.
[13] B. Mansoori, A. Mohammadi, S. Davudian, S. Shirjang, B. Baradaran, *Adv. Pharm. Bull.* **2017**, *7*, 339.
[14] W. Wislicenus, *Ber. Dtsch. Chem. Ges.* **1887**, *20*, 589.
[15] M. Matusi, R. Kimura, Y. Kubota, K. Funabiki, K. Manseki, J. Jin, A. Hansuebsai, Y. Inoue, S. Higashijima, *Dyes Pigm.* **2017**, *147*, 50.
[16] T. Du, R. Gao, Y. Deng, C. Wang, Q. Zhou, Y. Geng, *Angew. Chem. Int. Ed.* **2020**, *59*, 221.
[17] K. Shing, *Curr. Org. Synth.* **2016**, *13*, 385.
[18] S. Asadi, G. M. Ziarani, *Mol. Divers.* **2016**, *20*, 111.
[19] R. Pluskota, M. Koba, *Mini-Rev. Org. Chem.* **2018**, *18*, 1321.
[20] M. K. P. Jayatunga, S. Thompson, T. C. McKee, M. C. Chan, K. M. Reece, A. P. Hardy, R. Sekirnik, P. T. Seden, K. M. Cook, J. B. McMahon, W. D. Figg, C. J. Schofield, A. D. Hamilton, *Eur. J. Med. Chem.* **2015**, *94*, 509.
[21] B. E. Watt, A. T. Proudfoot, S. M. Bradberry, J. A. Vale, *Toxicol. Rev.* **2005**, *24*, 259.
[22] S. Amidi, F. Kobarfard, A. B. Moghaddam, K. Tabib, Z. Soleymani, *Iran. J. Pharm. Sci.* **2013**, *12*, 91.
[23] D. Leblois, S. Piessard, G. Le Baut, P. Kumar, J.-D. Brion, L. Sparfel, R.-Y. Sanches, M. Juge, J.-Y. Petit, L. Welin, *Eur. J. Med. Chem.* **1987**, *22*, 229.
[24] C. B. Mishra, A. Manral, S. Kumari, V. Saini, M. Tiwari, *Bioorg. Med. Chem.* **2016**, *24*, 3829.
[25] M. Jeyachandran, P. Ramesh, *Org. Chem. Int.* **2011**, 360810.
[26] R. Misra, R. C. Pandey, B. D. Hilton, *J. Antibiot.* **1987**, *40*, 786.
[27] Y. Wang, H.-X. Liu, Y.-C. Chen, Z.-H. Sun, H.-H. Li, S.-N. Li, M.-L. Yan, W.-M. Zhang, *Molecules* **2017**, *22*, 765.
[28] R. C. Pandey, M. W. Toussaint, R. M. Stroshane, C. C. Kalita, A. A. Aszalos, A. L. Garretson, T. T. Wei, K. M. Byrne, R. F. Geoghegan Jr., R. J. White, *J. Antibiot.* **1981**, *34*, 1389.
[29] D. J. Warnick-Pickle, K. M. Byrne, R. C. Pandey, R. J. White, *J. Antibiot.* **1981**, *34*, 1402.
[30] A. F. C. S. Oliveira, A. P. M. Souza, A. S. de Oliveira, M. L. da Silva, F. M. de Oliveira, E. G. Santos, I. E. P. da Silva, R. S. Ferreira, F. S. Villela, F. T. Martins, D. H. S. Leal, B. G. Vaz, R. R. Teixeira, S. O. de Paula, *Eur. J. Med. Chem.* **2018**, *149*, 98.
[31] R. P. Siqueira, M. M. M. Caetano, L. A. de Souza, P. M. S. dos Passos, N. B. Simaroli, M. V. A. Barros, A. P. M. de Souza, L. L. de Oliveira, A. Silva-Júnior, J. L. R. Fietto, R. R. Teixeira, F. R. Teixeira, G. C. Bressan, *Toxicol. In Vitro* **2020**, *65*, 104777.
[32] J. A. do Vale, A. P. M. de Souza, G. D. A. Lima, V. H. S. Gonçalves, G. A. Moreira, M. V. A. Barros, W. L. Pereira, N. C. L. Merchid, J. L. R. Fietto, G. C. Bressan, R. R. Teixeira, M. Machado-Neves, *Anticancer Drugs* **2020**, *31*, 718.
[33] R. R. Teixeira, A. M. da Silva, R. P. Siqueira, V. H. S. Gonçalves, H. S. Pereira, R. S. Ferreira, A. V. Costa, E. B. de Melo, F. R. Paula, M. M. C. Ferreira, G. C. Bressan, *J. Braz. Chem. Soc.* **2019**, *30*, 541.
[34] A. M. A. Lima, R. R. Teixeira, B. F. da Silva, R. P. Siqueira, I. E. P. da Silva, E. G. Santos, M. C. Fernandes, V. H. S. Gonçalves, G. C. Bressan, T. A. O. Mendes, S. O. de Paula, A. V. Costa, M. H. dos Santos, *Quim. Nova* **2019**, *42*, 473.
[35] M. C. F. Dias, B. L. de Sousa, M. Ionta, R. R. Teixeira, T. Q. Goulart, G. A. Ferreira-Silva, E. J. Pilau, M. H. dos Santos, *J. Braz. Chem. Soc.* **2021**, *32*, 572.
[36] P. A. R. Gazolla, R. R. Teixeira, A. M. da Silva, B. G. Vaz, G. A. Vasconcelos, R. P. Siqueira, V. H. S. Gonçalves, H. S. Pereira, G. C. Bressan, *Quim. Nova* **2018**, *41*, 497.
[37] G. D. A. Lima, M. P. Rodrigues, T. A. O. Mendes, G. A. Moreira, R. P. Siqueira, A. M. da Silva, B. G. Vaz, J. L. R. Fietto, G. C. Bressan, M. Machado-Neves, R. R. Teixeira, *Toxicol. In Vitro* **2018**, *53*, 1.
[38] G. A. Moreira, G. D. A. Lima, R. P. Siqueira, M. V. A. Barros, A. L. M. Adjanohoun, V. C. Santos, E. A. A. Barbosa, R. K. Loterio, J. C. de Paiva, V. H. S. Gonçalves, L. C. S. Viol, M. R. Almeida, J. L. R. Fietto, M. Machado-Neves, R. S. Ferreira, R. R. Teixeira, G. C. Bressan, *Toxicol. Appl. Pharmacol.* **2018**, *356*, 214.
[39] R. P. Siqueira, M. V. A. Barros, E. A. A. Barbosa, T. S. Onofre, V. H. S. Gonçalves, H. S. Pereira, A. S. Júnior, L. L. de Oliveira, M. R. Almeida, J. L. R. Fietto, R. R. Teixeira, G. C. Bressan, *Eur. J. Med. Chem.* **2017**, *134*, 97.
[40] A. F. S. Maia, R. P. Siqueira, F. M. O. de Oliveira, J. G. Ferreira, S. F. da Silva, C. A. D. Caiuby, L. L. de Oliveira, S. O. de Paula, R. A. C. Souza, S. Guilardi, G. C. Bressan, R. R. Teixeira, *Bioorg. Med. Chem. Lett.* **2016**, *26*, 2810.
[41] R. P. Siqueira, E. A. A. Barbosa, M. D. Polêto, G. L. Righetto, T. V. Seraphim, R. L. Salgado, J. G. Ferreira, M. V. A. Barros, L. L. de Oliveira, A. B. A. Laranjeira, M. R. Almeida, A. Silva-Júnior, J. L. R. Fietto, J. Kobarg, E. B. de Oliveira, R. R. Teixeira, J. C. Borges, J. A. Yunes, G. C. Bressan, *PLoS One* **2015**, *10*, e0134882.
[42] R. R. Teixeira, G. C. Bressan, W. L. Pereira, J. G. Ferreira, F. M. de Oliveira, D. C. Thomaz, *Molecules* **2013**, *18*, 1881.
[43] R. R. Teixeira, L. C. A. Barbosa, C. R. A. Maltha, M. E. Rocha, D. P. Bezerra, L. V. Costa-Lotufo, C. Pessoa, M. O. Moraes, *Molecules* **2007**, *12*, 1101.
[44] M. P. Rodrigues, D. C. Tomaz, L. A. de Souza, T. S. Onofre, W. A. de Menezes, J. Almeida-Silva, A. M. Suarez-Fontes, M. R. de Almeida, A. M. da Silva, G. C. Bressan, M. A. Vannier-Santos, J. L. R. Fietto, R. R. Teixeira, *Eur. J. Med. Chem.* **2019**, *183*, 111688.
[45] R. R. Teixeira, P. A. R. Gazolla, A. M. da Silva, M. P. G. Borsodi, B. R. Bergmann, R. S. Ferreira, B. G. Vaz, G. A. Vasconcelos, W. P. Lima, *Eur. J. Med. Chem.* **2018**, *146*, 274.
[46] W. L. Pereira, R. S. Vasconcellos, C. Mariotini-Moura, R. S. Gomes, R. C. Firmino, A. M. da Silva, A. Silva-Júnior, G. C. Bressan, M. R. Almeida, L. C. C. Afonso, R. R. Teixeira, J. L. R. Fietto, *Molecules* **2015**, *14*, 22435.
[47] H. N. Pati, U. Das, E. Clercq, J. Balzarini, J. R. Dimmock, *J. Enzyme Inhib. Med. Chem.* **2007**, *22*, 37.
[48] X. L. Liu, B. W. Pan, W. H. Zhang, C. Yang, J. Yang, Y. Shi, T. T. Feng, Y. Zhou, W. C. Yuan, *Org. Biomol. Chem.* **2014**, *13*, 601.
[49] O. Kouzi, E. Pontiki, D. Hadjipavlou-Litina, *Molecules* **2019**, *24*, 4411.
[50] H. Fadel, I. Sifaoui, A. López-Arencibia, M. Reyes-Batle, I. A. Jiménez, J. Lorenzo-Morales, N. Ghedadba, S. Benayache, J. E. Piñero, I. L. Bazzocchi, *Pathogens* **2019**, *8*, 201.
[51] S. B. Jannet, N. Hymery, S. Bourgou, A. Jdey, M. Lachaal, C. Magné, R. Ksouri, *Biomed. Pharmacother.* **2017**, *90*, 375.
[52] D. Lamorte, I. Faraone, I. Laurenzana, S. Trino, D. Russo, D. K. Rai, M. F. Armentano, P. Musto, A. Sgambato, L. D. De Luca, L. Milella, A. Caivano, *Molecules* **2020**, *25*, 4890.
[53] M. M. C. Ferreira, *J. Braz. Chem. Soc.* **2002**, *13*, 742.
[54] Guidance Document on the Validation of (Quantitative) Structure-Activity Relationship [(Q)SAR] Models. *OECD Environment Health*

and Safety Publications Series on Testing and Assessment No. 69, OECD, Paris **2007**. http://www.oecd.org/dataoecd/55/35/38130292.pdf (accessed: March 2017).
[55] L. Eriksson, J. Jaworska, A. P. Worth, M. T. Cronin, R. M. Mcdowell, P. Gramatica, *Environ. Health Persp.* **2003**, *111*, 1361.
[56] R. Kiralj, M. M. C. Ferreira, *J. Chemom.* **2010**, *24*, 681.
[57] K. Olympia, P. Eleni, H.-L. Dimitra, *Molecules* **2019**, *24*, 4411.
[58] S. Verma, A. K. Srivastava, O. P. Pandey, *PharmaTutor* **2018**, *6*, 22.
[59] M. C. A. Costa, P. O. M. Carvalho, M. M. C. Ferreira, *J. Chemom.* **2020**, *34*, e3131.
[60] K. W. Wellington, *Chem. Soc. Rev.* **2015**, *5*, 20309.
[61] T. Mosmann, *J. Immunol. Methods* **1983**, *65*, 55.
[62] Cambridge Crystallographic Data Centre, *Cambridge Structural Database Software Version 5.29-2007 + 1 Update*, Cambridge Crystallographic Data Centre, UK **2007**.
[63] F. Weigend, R. Ahlrich, *Phys. Chem. Chem. Phys.* **2005**, *7*, 3297.
[64] Gaussian 09, Revision A.02, M. J. Frisch, G. W. Trucks, H. B. Schlegel, G. E. Scuseria, M. A. Robb, J. R. Cheeseman, G. Scalmani, V. Barone, G. A. Petersson, H. Nakatsuji, X. Li, M. Caricato, A. Marenich, J. Bloino, B. G. Janesko, R. Gomperts, B. Mennucci, H. P. Hratchian, J. V. Ortiz, A. F. Izmaylov, J. L. Sonnenberg, D. Williams-Young, F. Ding, F. Lipparini, F. Egidi, J. Goings, B. Peng, A. Petrone, T. Henderson, D. Ranasinghe, V. G. Zakrzewski, J. Gao, N. Rega, G. Zheng, W. Liang, M. Hada, M. Ehara, K. Toyota, R. Fukuda, J. Hasegawa, M. Ishida, T. Nakajima, Y. Honda, O. Kitao, H. Nakai, T. Vreven, K. Throssell, J. A. Montgomery, Jr., J. E. Peralta, F. Ogliaro, M. Bearpark, J. J. Heyd, E. Brothers, K. N. Kudin, V. N. Staroverov, T. Keith, R. Kobayashi, J. Normand, K. Raghavachari, A. Rendell, J. C. Burant, S. S. Iyengar, J. Tomasi, M. Cossi, J. M. Millam, M. Klene, C. Adamo, R. Cammi, J. W. Ochterski, R. L. Martin, K. Morokuma, O. Farkas, J. B. Foresma, D. J. Fox, Gaussian Inc., Wallingford, CT **2016**.
[65] A. B. Nielsen, A. J. Holder, *GaussView 3.0 User's Reference*, Gaussian Inc., Pittsburgh, PA **2000**–2003.
[66] J. P. A. Martins, E. G. Barbosa, K. F. M. Pasqualato, M. M. C. Ferreira, *J. Chem. Inf. Model.* **2009**, *49*, 1428.
[67] E. Lindahl, B. Hess, D. van der Spoel, *J. Mol. Mod.* **2001**, *7*, 306.
[68] H. Kubinyi, *Drug Discov. Today* **1997**, *2*, 457.
[69] E. G. Barbosa, M. M. C. Ferreira, *Mol. Inf.* **2012**, *31*, 75.
[70] J. P. A. Martins, M. M. C. Ferreira, *Quim. Nova* **2013**, *36*, 554.
[71] R. F. Teófilo, J. P. A. Martins, M. M. C. Ferreira, *J. Chemom.* **2009**, *23*, 32.

SUPPORTING INFORMATION

Additional Supporting Information may be found online in the supporting information tab for this article.

How to cite this article: A. P. M. de Souza, M. C. A. Costa, A. R. de Aguiar, G. C. Bressan, G. D. de Almeida Lima, W. P. Lima, M. P. G. Borsodi, B. R. Bergmann, M. M. C. Ferreira, R. R. Teixeira, *Arch. Pharm.* 2021; e2100081. https://doi.org/10.1002/ardp.202100081